



## Microstructure Analysis of Mass Variations of LiOH/Cassava Peel Activated Carbon Nanocomposite

Lidya Agraini<sup>1</sup>, Yenni Darvina<sup>1,\*</sup>, Ramli<sup>1</sup>, Gusnedi<sup>1</sup>, Rahmat Hidayat<sup>1</sup>

<sup>1</sup> Department of Physics, Universitas Negeri Padang, Padang 25131, Indonesia

### Article History

Received : February, 10<sup>th</sup> 2024

Revised : February, 24<sup>th</sup> 2024

Accepted : March 31<sup>st</sup>, 2024

Published : March 31<sup>st</sup>, 2024

### DOI:

<https://doi.org/10.24036/jeap.v2i1.43>

### Corresponding Author

\*Author Name: Yenni Darvina

Email: [ydarvina@fmipa.unp.ac.id](mailto:ydarvina@fmipa.unp.ac.id)

**Abstract:** The lithium ion battery type rechargeable battery is widely used as an energy storage device. The advantages of using rechargeable batteries are practical and easy to carry everywhere and the disadvantages of rechargeable batteries is not able to work at high power. For this reason, it is necessary to conduct research on the forming material on the battery anode. This study was intended to characterize the structure, field and crystal size of the mass variation of LiOH/cassava peel activated carbon nanocomposite synthesized using the sol gel method with a mass variation ratio of 40%: 60%, 50% : 50%, and 60%: 40%. The LiOH/cassava peel activated carbon nanocomposite was mixed with PEG 6000 solution stirred at 100° C to form a gel which was dried and pulverized. XRD characterization was carried out and analyzed using High Score Plus software. Carbon has a cubic crystal structure with a diffraction peak of 29.41°. Activated carbon has a hexagonal crystal structure with diffraction peaks of 31.53° and 44.48°. The nanocomposite has a crystal structure that is hexagonal and orthorhombic for the carbon phase, while LiOH is monoclinic with different miller indices. The nanocomposite crystal size is 26.33 nm to 79.01 nm, with the smallest crystal size found when the LiOH/activated carbon nanocomposite variation is 40%: 60%. From the three comparisons, the more carbon the smaller the crystal size.

**Keywords:** Activated Carbon, Cassava Peel, LiOH, Nanocomposite, XRD



Journal of Experimental and Applied Physics is an open access article licensed under a Creative Commons Attribution ShareAlike 4.0 International License which permits unrestricted use, distribution, and reproduction in any medium, provided the original work is properly cited. ©2024 by author.

## 1. Introduction

The battery is one of the most reliable sources of electrical energy to operate portable or portable electronic equipment and is practical [1]. Portable electronic devices such as cellular phones (cell phones) and laptop computers continue to increase as material technology develops. Most of these electronic products, the energy system uses batteries [2]. Lithium batteries are the most widely used batteries in electronic equipment [3]. Lithium batteries are rechargeable

### How to cite:

L. Agraini, Y. Darfina, Ramli, Gusnedi and R. Hidayat, 2024, Microstructure Analysis of Mass Variations of LiOH/Cassava Peel Activated Carbon Nanocomposite, *Journal of Experimental and Applied Physics*, Vol.1, No.1, page 93-105.

batteries widely used for cell phones, laptops, digital cameras, and electric vehicles. [4]. Lithium-ion batteries have excellent power and energy, so they are capable of stable charging, so the use of Li-ion batteries in electric vehicles, micro-scale devices and large-scale equipment is increasing [5]. The advantages of lithium ion batteries are large power, high stability, resistance to high temperatures, economical, and more environmentally friendly [6]. The advantages of the battery system are simple, easy, and practical, also giving a more elegant feel. batteries can convert chemical energy into electrical energy by utilizing the reductionoxidation (redox) electrochemical reaction process [7].

The main component of the lithium ion battery anode is lithium. Lithium ( $\text{Li}^+$ ) in the form of Lithium Hydroxide ( $\text{LiOH}$ ) compound is a strong base and has an ionization degree of 1 or perfectly ionized. A perfectly ionized solution is a strong electrolyte solution and can conduct electric current well [8]. Lithium battery anode materials from activated carbon have been widely developed. Among them are from waste tires [9], hazelnut shells [10], nipah shells [11], and coconut shells [12]. The advantages of using activated carbon are that it has a large surface area, is stable, and is easily polarized. The manufacture of activated carbon from biomass has been widely done. Among them are the manufacture of carbon nanopores from coconut shell [13], the manufacture of nanocomposites from betung bamboo activated carbon [14], and the synthesis of electrodes from pepper skin carbon [15]. The use of  $\text{LiOH}$ /activated carbon nanocomposite as a lithium ion battery anode has been carried out using hazelnut shell activated carbon and tested for electrical properties in the form of capacitance and conductivity values [16].

Synthesis is an important part to obtain materials that have good recycling performance and capacity [17]. The synthesis of  $\text{LiOH}$ /activated carbon nanocomposites from cassava peels has not yet been carried out. The utilization of cassava peel waste so far is still not optimal, generally as animal feed, organic fertilizer, and processed food ingredients. Cassava peels contain high carbohydrates, indicating that the material also has a high elemental carbon content [18]. Cassava peels contain 59.31% C; 9.78% H; 28.74% O; 2.06% N; 0.11% S; 0.3% ash and 11.4%  $\text{H}_2\text{O}$  [19].

The incorporation of nanoparticles into matrix compositions is one of the developments in the world of technology. Nanocomposites are multiphase solid materials, where each phase has one, two, or three dimensions that are less than 100 nm or solid structures with nanometer-scale dimensions that repeat at different distances between structural forms [20]. One of the main advantages of nanocomposites is their ability to improve the performance of batteries and supercapacitors. An example of the application of nanocomposites is in the manufacture of lithium-ion batteries, electrode electrodes, where metal oxide and carbon nanocomposites can increase battery capacity, extend service life, and improve battery cycle stability [21].

The activated carbon has a pore size that is classified into three sizes, namely micropores have a diameter  $< 2$  nm, mesopores have a diameter of 2-50 nm, and macropores when the diameter is  $> 50$  nm [22]. The activated carbon is a porous solid consisting of 85-95% carbon, resulting from carbonaceous materials by heating them at high temperatures, using gas, water vapor, and chemicals so that the pores are open [23]. Activated carbon is classified into chemical products and not energy materials such as charcoal or charcoal briquettes that most of the pores of charcoal are still closed with hydrocarbons and organic compounds, while activated carbon is capable of adsorption because the surface is wider and the pores are open [24]. The characteristics of activated carbon are affected by the type of feedstock, surface area, pore distribution and surface chemistry of the charcoal, and the activation method used [25]. The

smaller the diameter of the carbon pores and the more pore volume, the bigger its surface area and absorbency of the carbon. This is greatly influenced by the process of carbonization and activation of carbon charcoal [26]. Activation will change the physical carbon where the surface area increases sharply because tar and residual charring compounds have disappeared [27].

Based on the above background, researchers doing research to see the microstructure of carbon, activated carbon, LiOH, and from the mass variation of LiOH nanocomposite/cassava peel activated carbon with different variations in the mass of LiOH: activated carbon used, namely 40%: 60%, 50% : 50%, and 60%: 40%. Characterization only uses XRD. The problems raised in this study are how is the microstructure in the form of structure, field and size of carbon, cassava peel activated carbon, and LiOH? And how is the effect of mass variation of LiOH/cassava peel activated carbon nanocomposite on the structure, plane and size of crystals?

## 2. Materials and Method

The research conducted is included in the category of experimental research on a laboratory scale by varying the mass of LiOH / Activated Carbon nanocomposites. This research discusses the microstructure analysis of LiOH/cassava peel activated carbon nanocomposite using XRD characterization. The research was doing from March to October 2023, at the Materials and Biophysics Laboratory, Department of Physics FMIPA, Padang State University, LLDIKTI Region X Padang City. The independent variables used are variations in the mass ratio of LiOH/activated carbon nanocomposite, namely: 40% : 60% ; 50% : 50%; and 60%: 40%. The dependent variable is the microstructure in the form of structure, plane and crystal size of carbon, cassava peel activated carbon, LiOH, and variations in the mass of LiOH/cassava peel activated carbon nanocomposite. While the control variables are the temperature and time of carbonization of cassava peel activated carbon, mass of activator, carbon activation time, temperature and heating time to become activated carbon powder, mass of PEG 6000, ethanol volume, temperature and time of stirring nanocomposite, mass of citric acid, and gel drying temperature.

Tools and materials used in the preparation of samples and data collection are porcelain cup, dropper, stirring rod, erlenmeyer, measuring cup, mortar and pestle, spatula, ph meter, filter paper, digital balance, petri dish, fume hood, desiccator, glass funnel, 230 mesh sieve, aluminum foil, *stainless steel*, furnace, oven, HEM, *Hot Plate Magnetic Stirrer*, XRD. The materials used are cassava peel, NaCl, LiOH, PEG 6000, citric acid, ethanol, and distilled water.

The preparation of activated carbon is made using chemical activation. Cassava peels are cleaned and then dried. then carbonized in a furnace at a temperature of 600° C for 2 hours. Then the charcoal is activated by soaking in a 5% NaCL solution for 1 hour at a temperature of 50° C while stirring using a *Hot Plate Magnetic Stirrer* with a rotating speed of 200 rpm then let stand for 24 hours [28]. Activated carbon is cleaned with filtered water until the pH is neutral and measured using a pH Meter then filtered using filter paper. The activated carbon obtained was dried in the oven at 110° C for 3 hours. Then the activated carbon was pulverized using HEM for 6 hours to produce nano size. The crushing using HEM is called the grinding technique, which is a crushing technique through a shaking system which makes the area of the sample surface wider with continuous collision energies occurring between the ball and the rotating bottle wall, resulting in a smaller size of the particle surface area [29]. Activated carbon from cassava peel is

mixed with LiOH (Lithium Hydroxide) to make nanocomposites and XRD characterization to see the microstructure in the form of structure, plane and crystal size. The preparation of LiOH/cassava peel activated carbon nanocomposites was carried out using the sol gel method. The sol gel method is a process used to make inorganic materials through a chemical reaction in a solution at relatively low temperatures. The process begins by mixing metals or salts in water or a suitable solvent, such as alcohol at room temperature or low temperature. Then XRD characterization was carried out. Here is a picture of activated carbon that has been dried in the oven. The shape of activated carbon can be viewed in Figure 1 below:

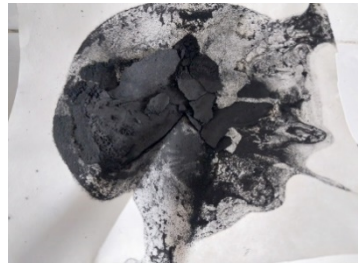


Figure 1. Activated carbon

Figure 1 shows the oven-dried activated carbon sample ready to be used as a nanocomposite material. Preparation of nanocomposites performed using the sol gel method [16]. Raw materials in the form of LiOH/active carbon nanocomposite powder with a mass composition variation ratio of 40%: 60% ; 50% : 50%; and 60%: 40% with a total mass of 3 g mixed, stirred and crushed until homogeneous. A total of 45 g of PEG 6000 was put into a measuring cup and dissolved with 60 mL of 95% ethanol at a temperature of 50° C while stirring using a *Hot Plate Magnetic Stirrer* until homogeneous then 4 molar citric acid was added to pH 4-5 (acidic). The stirring temperature was increased to 100° C for 1 hour to form a gel and wait until dry. The dried gel was pulverized using mortal and pestle. The shape of the nanocomposite gel can be viewed in Figure 2 below:

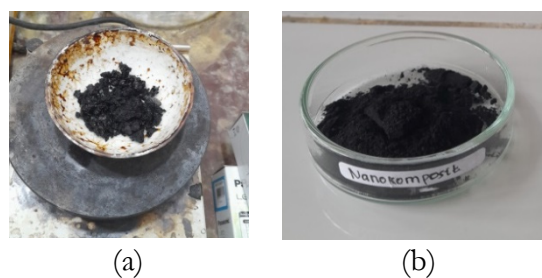


Figure 2. (a) nanocomposite gel dried and (b) pulverized nanocomposite.

Based on Figure 2, it can be viewed that the nanocomposite gel was dried using a *hot plate* and then smoothed. After that, characterization is carried out using XRD. The X-ray diffraction can also be used to measure the size of crystals with a particular phase [30]. The X-ray diffraction is an analytical method that utilizes the interaction between X-rays and atoms arranged in a crystal structure [31]. The crystallite dimension can be calculated based on the modified Debye Scherrer formula that uses the wavelength, intensity, diffraction angle  $2\theta$  and FWHM values that have been produced from the XRD analysis. The Debye Scherrer equation can show that the resulting crystal size value will be inversely related to the FWHM value, while the FWHM value is

influenced by the intensity of each crystal plane, which is the higher the intensity, the lower the FWHM value [32]. The definition refers to the major peaks in the diffractogram pattern through the Debye Scherrer equation approach formulated as follows:

$$D = K \frac{\lambda}{\beta \cos \theta} \quad (1)$$

Description:

D= crystal size

K= shape factor of the crystal (0.9-1)

$\lambda$  = wavelength of X-ray (1.54056 Å)

$\beta$  = value of Full Width at Half Maximum (FWHM) (rad)

$\theta$  = diffraction angle (degree)

### 3. Results and Discussion

Carbon was made using the carbonization method at 600° C for 2 hours. The solid material that remains after carbonization is carbon in the form of charcoal with narrow pores [33]. The manufacture of activated carbon is done using chemical activation. Chemical activation in principle is the soaking of charcoal with chemical compounds before heating [34]. The activator used is 5% NaCL. The activated carbon was then characterized using XRD. The results of testing carbon and cassava peel activated carbon can be seen in Figure 3 in the form of diffractograms that produce intensity peaks along the 2 $\theta$  angle.

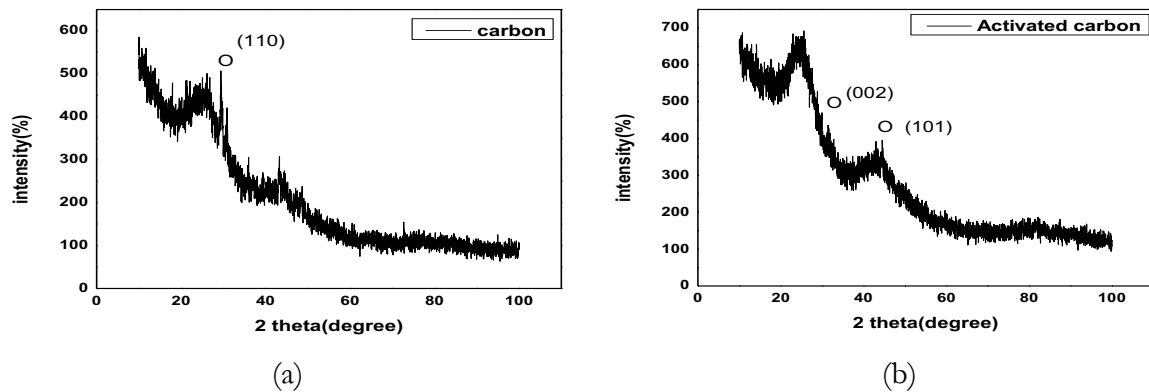


Figure 3. (a) cassava peel carbon and (b) cassava peel activated carbon

Based on Figure 3, the resulting diffractogram has a relationship between the intensity and angle of diffraction (2 $\theta$ ), and also produces the value of the distance between planes (d) and full width at half maximum (FWHM). The values can be viewed in Table 1 below:

Table 1. Diffractogram data of carbon and cassava peel activated carbon

| Pos.[°2 $\theta$ ] | d-spacing[Å] | Ir[%] | FWHM Left[°2 $\theta$ ] | Description |
|--------------------|--------------|-------|-------------------------|-------------|
| 29,41              | 3,033683     | 100   | 0,153504                | Carbon      |
| 31,54              | 2,83669      | 100   | 0,818688                | Activated   |

|       |         |   |          |        |
|-------|---------|---|----------|--------|
| 44,48 | 2,03511 | 3 | 0,614016 | carbon |
|-------|---------|---|----------|--------|

Table 1 is the result of XRD characterization analysis using *High Score Plus* software. In the cassava peel carbon sample, there is a diffraction peak at a diffraction angle of  $29.41^\circ$  with a miller index (110). Furthermore, in the cassava peel activated carbon sample there are diffraction peaks at diffraction angles of  $31.54^\circ$  and  $44.48^\circ$  with miller indices (002) and (101). The addition of peaks is seen when the carbon has been activated. Previous research on cassava peel activated carbon diffraction peaks are at  $21^\circ$ ,  $22^\circ$  and  $24^\circ$  with miller index (002),  $43^\circ$ ,  $44^\circ$  and  $48^\circ$  diffraction peaks with miller index (110) [35]. The carbon lattice constant is found when the value of  $a = b = c = 4.28$  (Å) with angles  $\alpha = \beta = \gamma = 90^\circ$  which produces a cubic crystal structure. While the lattice constant of activated carbon is found when the values of  $a = 2.46$  (Å),  $b = 2.46$  (Å), and  $c = 6.73$  (Å) with angles  $\alpha = \beta = 90^\circ$ , and  $\gamma = 120^\circ$  which produces a hexagonal crystal structure... The results of the *High Score Plus* software analysis produced the diffraction angle and FWHM values used to determine the crystal size of carbon and cassava peel activated carbon, where the values can be viewed in Table 2 below:

Table 2. Crystal size values of carbon and cassava peel activated carbon

| K   | $\lambda$ (nm) | $\beta$ (rad) | $\theta$ ( $^\circ$ ) | D (nm) | Description |
|-----|----------------|---------------|-----------------------|--------|-------------|
| 0,9 | 0,154          | 0,001338896   | 14,70619              | 107,02 | Carbon      |
| 0,9 | 0,154          | 0,007140779   | 15,76982              | 20,17  | Activated   |
| 0,9 | 0,154          | 0,005355584   | 22,24116              | 27,96  | carbon      |

Based on Table 2, the value of carbon crystal size is 107.02 nm, while activated carbon is 20.17 nm and 27.96 nm. Carbon mostly has pores that are still covered with hydrocarbons and organic compounds, while activated carbon has a wider surface and pores [23]. Characterization of materials in the form of LiOH can be seen in Figure 4 below in the form of diffractograms that produce intensity peaks along the  $2\theta$  angle of 10-100 $^\circ$ .

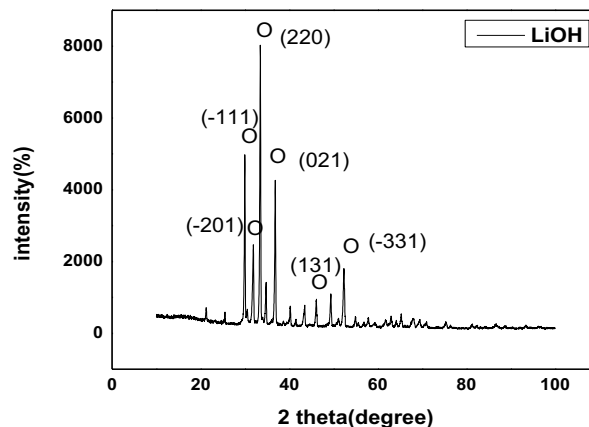


Figure 4. LiOH characterization results

Based on Figure 4, the resulting diffractogram has a relationship between the intensity and angle of diffraction ( $2\theta$ ), and also produces the value of the distance between planes ( $d$ ) and full width at half maximum (FWHM). The values can be viewed in Table 3 below:

Table 3. LiOH Characterization Results

| Pos.[ $^{\circ}2\theta$ ] | d-spacing[ $\text{\AA}$ ] | Ir[%] | FWHM<br>Left[ $^{\circ}2\theta$ ] |
|---------------------------|---------------------------|-------|-----------------------------------|
| 29.98                     | 2.98041                   | 60.39 | 0.179088                          |
| 31.89                     | 2.80565                   | 27.84 | 0.179088                          |
| 34.76                     | 2.58098                   | 15.51 | 0.153504                          |
| 36.85                     | 2.43947                   | 53.18 | 0.204672                          |
| 49.39                     | 1.84506                   | 11.69 | 0.179088                          |
| 52.32                     | 1.74866                   | 21.37 | 0.179088                          |

In Table 3, there are diffraction peaks at diffraction angles of 29.98 $^{\circ}$ , 31.89 $^{\circ}$ , 34.76 $^{\circ}$ , 36.85 $^{\circ}$ , 49.39 $^{\circ}$ , and 52.32 $^{\circ}$  with miller indices (-111), (-201), (220), (021), (131), and (-331). The LiOH lattice constant is found when the value of  $a = 7.41$  ( $\text{\AA}$ ),  $b = 8.30$  ( $\text{\AA}$ ), and  $c = 3.19$  ( $\text{\AA}$ ) with angles  $\alpha = \gamma = 90^{\circ}$ ,  $\beta = 110^{\circ}$  which produces a monoclinic crystal structure. The results of the *High Score Plus* software analysis produce the diffraction angle and FWHM values used to determine the size of the LiOH crystal, where the values can be viewed in Table 4 below:

Table 4. LiOH crystal size

| K   | $\lambda$ (nm) | $\beta$ (rad) | $\theta(^{\circ})$ | D (nm) |
|-----|----------------|---------------|--------------------|--------|
| 0,9 | 0,154          | 0.001562045   | 14.99105           | 91.85  |
| 0,9 | 0,154          | 0.001562045   | 15.94893           | 92.28  |
| 0,9 | 0,154          | 0.001338896   | 17.37953           | 108.47 |
| 0,9 | 0,154          | 0.001785195   | 18.42281           | 81.83  |
| 0,9 | 0,154          | 0.001562045   | 24.6982            | 97.66  |
| 0,9 | 0,154          | 0.001562045   | 26.15964           | 98.85  |

Based on Table 2, the crystal size values of LiOH are 91.85 nm, 92.28 nm, 108.47 nm, 81.83 nm, 97.66 nm, and 98.85 nm. After XRD characterization of the material and its crystal size value  $< 100$  nm, it is qualified as a nanocomposite material. After that, the LiOH/cassava peel activated carbon nanocomposite was made.

Formation of LiOH/cassava peel activated carbon nanocomposite using sol gel method with nanocomposite mass variation of 40%: 60%, 50% : 50%, and 60%: 40%. The nanocomposites were then subjected to XRD characterization. The results of the LiOH nanocomposite characterization test: Activated carbon variation 40%: 60% variation can be seen in Figure 5, which is a diffractogram that produces intensity peaks along the  $2\theta$  angle.

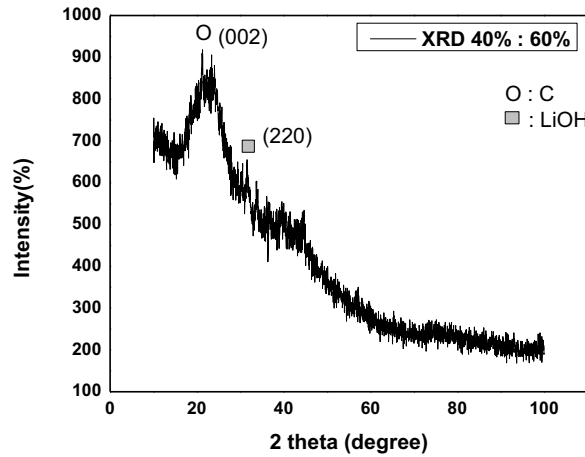


Figure 5. Nanocomposite diffractogram of 40%: 60%

Based on Figure 5, the resulting diffractogram has a relationship between the intensity and angle of diffraction ( $2\theta$ ), and also produces the value of the distance between planes ( $d$ ) and full width at half maximum (FWHM). The values can be viewed in Table 5 below:

Table 5. Characterization Results XRD of variation 40%: 60%

| Pos.[ $^{\circ}2\theta$ ] | d-spacing[ $\text{\AA}$ ] | Ir[%] | FWHM<br>Left[ $^{\circ}2\theta$ ] | hkl | Phase |
|---------------------------|---------------------------|-------|-----------------------------------|-----|-------|
| 21.17                     | 4.19655                   | 100   | 0.614016                          | 002 | C     |
| 33.77                     | 2.65418                   | 100   | 0.614016                          | 220 | LiOH  |

Table 5 is the result of XRD characterization analysis using *High Score Plus* software. In the variation 40%: 60% variation, there is a diffraction peak at a diffraction angle of  $21.17^{\circ}$  for the carbon phase and  $33.77^{\circ}$  for the LiOH phase with miller indices (002) and (220). The carbon lattice constant is found when the value of  $a = b = 2.47$  ( $\text{\AA}$ ), and  $c = 6.72$  ( $\text{\AA}$ ) with angles  $\alpha = \beta = 90^{\circ}$  and  $\gamma = 120^{\circ}$  which produces a Hexagonal crystal structure. While the LiOH lattice constant when the value of  $a = 6.95$  ( $\text{\AA}$ ),  $b = 8.28$  ( $\text{\AA}$ ), and  $c = 3.20$  ( $\text{\AA}$ ) with angles  $\alpha = 90^{\circ}$ ,  $\beta = 95^{\circ}$ , and  $\gamma = 90^{\circ}$  and produces a monoclinic crystal structure. The results of the *High Score Plus* software analysis produce diffraction angle and FWHM values which are used to determine the size of the nanocomposite crystals. In Table 6 below, the carbon crystal size is  $26.33^{\circ}$  and LiOH  $27.05^{\circ}$ .

Table 6. Crystal size results of LiOH/activated carbon nanocomposite 40% : 60%

| K   | $\lambda$ (nm) | $\beta$ (rad) | $\theta$ ( $^{\circ}$ ) | D (nm) |
|-----|----------------|---------------|-------------------------|--------|
| 0,9 | 0,154          | 0,005355584   | 10,58579                | 26,33  |
| 0,9 | 0,154          | 0,005355584   | 16,88557                | 27,05  |

LiOH nanocomposite characterization test results: Activated carbon variation 50%: 50% variation can be seen in Figure 6, which is a diffractogram that produces intensity peaks along the  $2\theta$  angle.



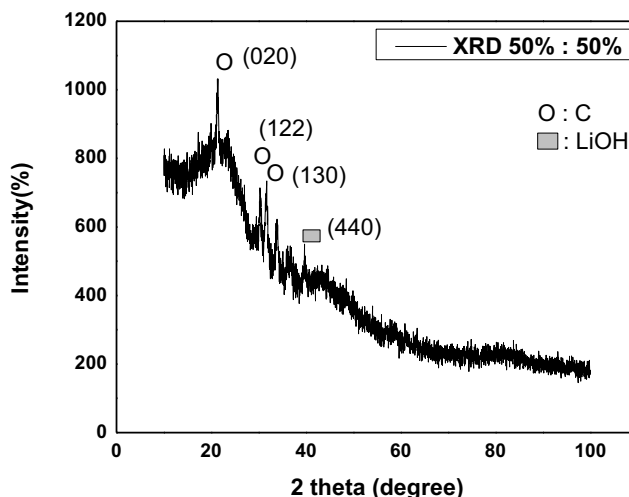


Figure 6. nanocomposite diffractogram 50% : 50%

Based on Figure 6, the resulting diffractogram has a relationship between the intensity and angle of diffraction ( $2\theta$ ), and also produces the value of the distance between planes ( $d$ ) and full width at half maximum (FWHM). The values can be viewed in Table 7 below :

Table 7. XRD Characterization Results of variation 50% : 50%

| Pos.[ $^{\circ}2\theta$ ] | d-spacing[ $\text{\AA}$ ] | Ir[%] | FWHM Left[ $^{\circ}2\theta$ ] | Hkl | Phase |
|---------------------------|---------------------------|-------|--------------------------------|-----|-------|
| 21.29                     | 4.17252                   | 82.1  | 0.307008                       | 020 | C     |
| 30.38                     | 2.94194                   | 72.34 | 0.358176                       | 122 | C     |
| 31.63                     | 2.8281                    | 100   | 0.51168                        | 130 | C     |
| 33.93                     | 2.64144                   | 100   | 0.460512                       | 440 | LiOH  |

Table 7 is the result of XRD characterization analysis of variation nanocomposite 50%: 50% variation, there are diffraction peaks at diffraction angles of 21.29°, 30.38°, 31.63° for the carbon phase while the LiOH phase is found at a peak of 33.93°. The carbon phase has miller indices (020), (122), and (130), for the LiOH phase (440). The carbon lattice constant is found when the value of  $a = 9.53$  ( $\text{\AA}$ ),  $b = 8.87$  ( $\text{\AA}$ ), and  $c = 8.34$  ( $\text{\AA}$ ) with angles  $\alpha = \beta = \gamma = 90^{\circ}$  which produces an Orthorhombic crystal structure. While the LiOH lattice constant when the value of  $a = 7.37$  ( $\text{\AA}$ ),  $b = 8.26$  ( $\text{\AA}$ ), and  $c = 3.19$  ( $\text{\AA}$ ) with angles  $\alpha = \gamma = 90^{\circ}$ , and  $\beta = 110^{\circ}$  which produces a monoclinic crystal structure. The results of the *High Score Plus* software analysis produce the diffraction angle and FWHM values used to determine the size of the nanocomposite crystal, where the values can be viewed in Table 8 below:

Table 8. Crystal size results of LiOH/activated carbon nanocomposite 60% : 40%

| K   | $\lambda$ (nm) | $\beta$ (rad) | $\theta$ (°) | D (nm) |
|-----|----------------|---------------|--------------|--------|
| 0,9 | 0,154          | 0,002677792   | 10,64745     | 52,66  |
| 0,9 | 0,154          | 0,003124091   | 15,19179     | 45,97  |
| 0,9 | 0,154          | 0,004462987   | 15,81896     | 32,27  |
| 0,9 | 0,154          | 0,004016688   | 16,96949     | 36,07  |

Based on Table 8, the crystal sizes obtained in the variation 60% : 40% variation are 52.66nm, 45.97 nm, 32.27 nm for the carbon phase, while the LiOH phase has a size of 36.07 nm. Characterization test results of LiOH/Activated carbon nanocomposites variation 60%: 40% variation can be seen in Figure 7, which is a diffractogram that produces intensity peaks along the  $2\theta$  angle.

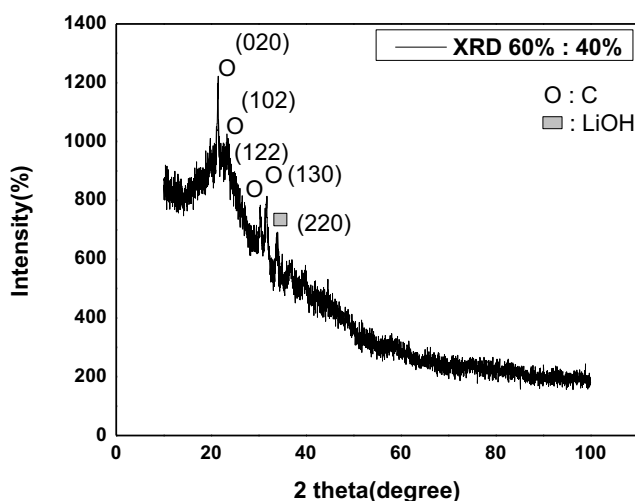


Figure 7. nanocomposite diffractogram 60% : 40%

Based on Figure 7, the resulting diffractogram has a relationship between the intensity and angle of diffraction ( $2\theta$ ), and also produces the value of the distance between planes (d) and full width at half maximum (FWHM). The values can be viewed in Table 9 below:

Table 9. XRD Characterization Results of variation 60% : 40%

| Pos.[°2 $\theta$ ] | d-spacing[Å] | Ir[%] | FWHM Left[°2 $\theta$ ] | hkl | Phase |
|--------------------|--------------|-------|-------------------------|-----|-------|
| 21.43              | 4.14615      | 100   | 0.204672                | 020 | C     |
| 23.52              | 3.78235      | 31.67 | 0.614016                | 102 | C     |
| 30.43              | 2.9371       | 41.32 | 0.409344                | 122 | C     |
| 31.69              | 2.82324      | 68.54 | 0.358176                | 130 | C     |
| 33.92              | 2.64264      | 100   | 0.409344                | 220 | LiOH  |

Table 9 is the result of XRD characterization analysis of nanocomposite variation 60%: 40% variation, there are diffraction peaks at diffraction angles of 21.43°, 23.52°, 30.43°, and 31.69° for

the carbon phase while the LiOH phase is found at a peak of 33.77°. The carbon phase has miller indices (020), (102), (122), and (130), for the LiOH phase (220). The carbon lattice constant is found when the value of  $a = 9.53$  (Å),  $b = 8.87$  (Å), and  $c = 8.34$  (Å) with angles  $\alpha = \beta = \gamma = 90^\circ$  which produces an Orthorhombic crystal structure. While the LiOH lattice constant when the value of  $a = 6.95$  (Å),  $b = 8.28$  (Å), and  $c = 3.20$  (Å) with angles  $\alpha = \gamma = 90^\circ$ , and  $\beta = 95^\circ$  which produces a monoclinic crystal structure. The results of the *High Score Plus* software analysis produce the diffraction angle and FWHM values used to determine the size of the nanocomposite crystal, where the values can be viewed in Table 10 below:

Table 10. Crystal size results of LiOH/activated carbon nanocomposite 60%: 40%

| K   | $\lambda$ (nm) | $\beta$ (rad) | $\theta$ (°) | D (nm) |
|-----|----------------|---------------|--------------|--------|
| 0,9 | 0,154          | 0,001785195   | 10,71598     | 79,01  |
| 0,9 | 0,154          | 0,005355584   | 11,76073     | 26,43  |
| 0,9 | 0,154          | 0,003570389   | 15,21740     | 40,23  |
| 0,9 | 0,154          | 0,003124091   | 15,84695     | 46,12  |
| 0,9 | 0,154          | 0,003570389   | 16,96157     | 40,58  |

Based on Table 10, the crystal sizes obtained in the variation 60% : 40% variation are 79.01 nm, 26.43 nm, 40.23 nm, and 46.12 nm for the carbon phase, while the LiOH phase has a crystallite size of 40.58 nm. From the results obtained, the crystal size value of LiOH/cassava peel activated carbon nanocomposite is between 26 nm to 79 nm. This is in accordance with the theory that nanocomposites have a crystal size of less than 100 nm. The change in angle and decrease in diffraction intensity indicate that during the carbonization process the chemical compounds in cassava peel carbon began to degrade, but have not yet changed the crystallite structure. From the three variations of nanocomposites, the resulting diffractogram has almost the same peak, namely the peak between 21° and the peak between 31°. The peak between 21° and the peak between 31° indicates the presence of amorphous solid structures where amorphous materials are formed from natural materials [36]. Diffraction peaks that are blunt with low diffraction intensity on X-ray diffractograms indicate the presence of material structures with low levels of crystallinity or amorphous materials, where the amount of amorphous phases formed on X-ray diffractograms is generally directly related to the amount of mesoporous structures contained in the material being analyzed [37] [38]. In previous research with the synthesis of LiOH/activated carbon shell hazelnut nanocomposites the crystal size gets bigger as the mass concentration of LiOH increases [29]. This is in accordance with the research that has been done on LiOH/cassava peel activated carbon nanocomposites, the higher the mass of LiOH, the greater the crystal size value, namely in the variation 60% : 40%.

## 4. Conclusion

The crystal structure of cassava peel carbon is cubic, cassava peel activated carbon is hexagonal, and LiOH is monoclinic. The carbon nanocomposite has orthorhombic and hexagonal structures, while LiOH is monoclinic. The mass variation of LiOH/cassava peel activated carbon nanocomposite 40% : 60% has a smaller crystal size. This indicates that when the composition of carbon is more than LiOH, it will minimize the crystal size.

## Acknowledgments

This research can be completed well thanks to the help of various people. Therefore, the authors would like to express their gratitude to the higher education service institution region x (LLDIKTI X), as well as the research team who have participated in this research.

## References

- [1] M. Nasution, "Karakteristik Baterai Sebagai Penyimpan Energi Listrik Secara Spesifik," *JET (Journal Electr. Technol.*, vol. 6, no. 1, pp. 35–40, 2021
- [2] Y. Wang, B. Liu, Q. Li, S. S. Ferrara, Z. D. Deng, J. Xiao. "Lithium and Lithium Ion Batteries for Applications in Microelectronic Devices: A Review". *J. of Power Sources*, vol. 286, pp. 330-345, 2015
- [3] V. Sahanaya, Ramli, and Y. Darvina, "Pengaruh Fraksi Konsentrasi Nanokomposit Fe<sub>3</sub>O<sub>4</sub>/PANi dengan Metode Sol-Gel Spin Coating untuk Material Elektroda Baterai Lithium," *Pillar Phys.*, vol. 11, no. 2, pp. 49–56, 2018.
- [4] U. Wietelmann and R.J. Bauer, "Lithium and Lithium Compounds. Ullmann's Encyclopedia of Industrial Chemistry". doi:10.1002/14356007.a15\_393. ISBN 3-527-30673-0.2000
- [5] W. Xie, Y. Dang, L. Wu, W. Liu, A. Tang, and Y. Luo, "Experimental and Molecular Simulating Study on Promoting Electrolyte Immersed Mechanical Properties of Cellulose/Lignin Separator for Lithium-Ion Battery," *Polym Test*, vol. 90, 2020
- [6] L. Lu Han, X. Li, J. Hua, J. and Ouyang, M, "A Review on The Key Issues for Lithium-Ion Battery Management in Electric Vehicles", *J. Power Sources*, vol. 226, pp. 272–288, 2013
- [7] Y. Matsuo, R. Kostecki, and F. Mc Larnon. "Surface Layer Formation on Thin-Film LiMn<sub>2</sub>O<sub>4</sub> Electrodes at Elevated Temperatures". *J. Electrochem. Soc.*, vol. 148, pp.A687-A692, 2001.
- [8] K. Poppy, S. Setiasih & A. Sidharta, "Larutan Asam, Basa, Dan Garam", Departemen Pendidikan Nasional: Bandung, 2007
- [9] F. A. Mumtahirah, "Pembuatan Karbon Aktif dari Limbah Ban Bekas dengan Metode Pirolisis Sebagai Material Anoda Baterai Lithium-Ion." 2023
- [10] V. S. I. Negara, "Pengaruh Temperatur Sintering Karbon Aktif Berbasis Tempurung Kemiri Terhadap Sifat Listrik Anoda Baterai Litium", *Jurnal Fisika Unand*, vol. 4, no. 2, pp. 178–184, 2015.
- [11] T. Evila, P. Sri, M. Nurhilal, and R. Dwityaningsih, "Analisis Porositas, Tekstur, dan Morfologi Karbon Tempurung Nipah Hasil Pirolisis Suhu Tinggi untuk Anoda Baterai Sekunder," vol. 14, no. 01, pp. 119–129, 2023, doi: 10.35970/infotekmesin.v14i1.1666.
- [12] N. Nursanti, "Penentuan Kapasitansi Spesifik Karbon Aktif Tempurung Kelapa (Cocos nucifera L) Hasil Modifikasi dengan HNO<sub>3</sub>, H<sub>2</sub>SO<sub>4</sub> DAN H<sub>2</sub>O<sub>2</sub> Menggunakan Metode Cyclic Voltammetry (CV)" (Doctoral dissertation, Universitas Hasanuddin), 2017
- [13] M. Rosi, F. Iskandar, and M. Abdullah, "Sintesis Nanopori Karbon dengan Variasi Jumlah NaOH dan Aplikasinya sebagai Superkapasitor Sintesis Nanopori Karbon dengan Variasi Jumlah NaOH dan Aplikasinya sebagai Superkapasitor," *Semin. Nas. Fis. Inst. Teknol. Bandung*, pp. 74–77, 2013.
- [14] A. Aflahannisa and Astuti, "Sintesis Nanokomposit Karbon-TiO<sub>2</sub> Sebagai Anoda Baterai Lithium," vol. 5, no. 4, pp. 357–363, 2016.
- [15] N. Maryati, "Sintesis Elektroda Anoda Baterai Ion Lithium Berbasis Karbon Aktif Kulit Lada", Skripsi. Universitas Bangka Belitung, 2021

- [16] H. Susana and Astuti, "Pengaruh Konsentrasi LiOH Terhadap Sifat Listrik Anoda Baterai Lithium Berbasis Karbon Aktif Tempurung Kemiri", *5(2)*, 136–141, 2016.
- [17] S.T. Myung, K. Amine, Y.K. Sun. "Review: Nanostructured Cathode Materials for Rechargeable Lithium Batteries". *J. of Power Sources*, vol. 283, pp. 219-236, 2015.
- [18] S. Utomo, "Pengaruh Waktu Aktivasi dan Ukuran Partikel Terhadap Daya Serap Karbon Aktif dari Kulit Singkong dengan Aktivator NaOH", *Prosiding Seminar Nasional Sains dan teknologi*. Universitas Muhammadiyah Jakarta, Indonesia, 2014
- [19] Ikawati and M. Melati, "Pembuatan Karbon Aktif dari Kulit Singkong UKM Tapioka Kabupaten Pati," pp. 1–8, 2010
- [20] Rahmi, Ramli, and Y. Darvina, " Analisis Sifat Listrik Nanokomposit Fe<sub>3</sub>O<sub>4</sub>/PVDF yang disintesis dengan Metode Sol Gel untuk Aplikasi Elektroda Baterai Lithium Ion", *Pillar Phys.*, vol. 11, no. 2, pp. 73–80, 2018.
- [21] L. M. Manocha., J. Valand., N. Patel, A. Warriar, & Manocha, S, "Nanocomposites for Structural Applications", In *Indian Journal of Pure & Applied Physics*(Vol. 44),2006
- [22] J.W. Hessler, "Active Carbon", Chemical Publishing Co Inc., Boston (MA), 1951
- [23] L. Maulinda, N. Za, D. N. Sari, J. T. Kimia, F. Teknik, and U. Malikussaleh, "Jurnal Teknologi Kimia Unimal Pemanfaatan Kulit Singkong sebagai Bahan Baku Karbon Aktif," vol. 2, no. November, pp. 11–19, 2015.
- [24] E.S. Harsanti and A. N. Ardiwinata, " Arang Aktif Meningkatkan Kualitas Lingkungan Sinar Tani ", *Edisi 6-12 : 10-12*. Jakarta: Badan Litbang Pertanian, 2001
- [25] G.T. Austin, "Shreve's Chemical Process Industry, Fifth Edition", McGraw Hill Book Company, Newyork, hal 136-138., 1984
- [26] W. Satriady., A. H. I. Alamsyah, Saad, and S. Hidayat, "Pengaruh Luas Elektroda Terhadap Kartakteristik Baterai LiFePO<sub>4</sub>", *J. Mater. dan Energi Indonesia*, vol. 06, no. 02, pp. 43–48, 2016
- [27] M. Elma, "Proses Sol Gel: Analisis , Fundamental dan Aplikasi", *Universitas Lambung Mangkurat : Lambung Mangkurat University Press*, 2018
- [28] A. R. Permatasari, L. U. Khasanah, and E. Widowati, "Karakterisasi Karbon Aktif Kulit Singkong ( Manihot utilissima ) dengan Variasi Jenis Aktivator", *Vol. VII*, no. 2, pp. 70–75, 2014.
- [29] Aminatun, A. Supardi, Z. I. Nisa, D. Hikmawati, and Siswanto, "Synthesis of Nanohydroxyapatite from Cuttlefish Bone (*Sepia sp.*) Using Milling Method," *Int. J. Biomater.*, vol. 2019, 2019, doi: 10.1155/2019/1831208.
- [30] West and R. Anthony, "Solid State Chemistry and Its Application", New York: John Wiley And Sons, 1989
- [31] A. Setiabudi., R. Hardian, and Muzakir, A, " Karakterisasi Material", Universitas Pendidikan Indonesia : UPI PRESS, 2012
- [32] A.B. Masruroh., Manggara., T. Lapailaka., and R.T. Triandi, "Penentuan Ukuran Kristal (Crystallite Size) Lapisan Tipis Pzt dengan Metode Xrd Melalui Pendekatan Persamaan Debye Scherrer", Fakultas Matematika Dan Ilmu Pengetahuan Alam, Malang, Universitas Brawijaya, 2014
- [33] N.P. Cheremisinoff, "Carbon Adsorptionfor Pollution Control", Prentice Hall. Englewood Cliffs, NJ. USA, 1993
- [34] M. Lempang, "Pembuatan dan Kegunaan Arang Aktif", *Info Teknis EBONI*. 11 (2): 65-80, 2014
- [35] T.M. Situmorang and R. Farma, "Pengaruh Aktivator Kimia Terhadap Kualitas Karbon Aktif dari Kulit Singkong Sebagai Bahan Penyerap Logam Berat", Fakultas Matematika dan Ilmu Pengetahuan Alam, Riau, Universitas Riau, 2017
- [36] R.Aarthi, a. K, "Influence of Chemical Reactions Over The Formation of Graphene Oxide Nanoparticles", *Rasāyan J. Chem. Vol. 7 no. 4*, 340-342, 2014
- [37] D. Prasetyoko., I. Purnamasari and D. Hartanto, "Esterifikasi Asam Lemak Stearin Kelapa Sawit Menggunakan Katalis H-ZSM-5 Mesopori yang disintesis Dengan Metode Nanoprekursor", *Seminar Nasional Zeolit VII*. 2011 October 17-18; Surabaya, Indonesia, 2011
- [38] D. Hartanto., T.E. Purbaningtiyas., H. Fansuri and D. Prasetyoko, "Karakterisasi Struktur Pori dan Morfologi ZSM-2 Mesopori yang disintesis dengan Variasi Waktu Aging", *J Ilmu Dasar*. 12 (1): 80-90. 2011